Decentralized Voltage Control of Boost Converters in DC Microgrids: Feasibility Guarantees

Morteza Nazari Monfared, Yu Kawano, *Member, IEEE*, and Michele Cucuzzella, *Member, IEEE*

***Abstract*— This article deals with the design of a decentralized dynamic control scheme to regulate the voltage of a direct current (dc) microgrid composed of boost converters supplying unknown loads. Moreover, the proposed control scheme guarantees that physical system constraints are satisfied at each time instant. Specifically, we guarantee that the voltages evolve in the positive orthant and that the duty cycle of each boost converter remains within specified bounds. The control design is based on Lyapunov theory and, more precisely, we use a Krasovskii Lyapunov function to estimate a feasible domain of attraction of the closed-loop system. Then, we guarantee that for any initial condition inside the estimated domain of attraction, the desired equilibrium point is asymptotically stable and the physical constraints are satisfied at each time instant. Finally, we assess the effectiveness of the proposed control scheme through extensive and realistic simulation scenarios.**

***Index Terms*— Decentralized control, direct current (dc) microgrids, Lyapunov methods, nonlinear systems, voltage regulation.**

I. Introduction

DRIVEN by economic, technological, and environmental factors, the key challenge in power grids currently involves shifting from traditional power generation and transmission systems to integrating smaller distributed generation units (DGUs) [1]. In addition, the escalating energy demand and public concern over global warming have spurred efforts toward adopting eco-friendly renewable energy sources (RESs) [2], which are essential to reduce CO_2 emissions and decrease fossil fuel reliance, enhance energy efficiency by minimizing power losses, and cut costs for electrifying remote areas or increasing the capacity of existing grids to meet the rising electricity demand. However, the adoption and integration of DGUs necessitate substantial changes to conventional power systems [3], which led to the notion and development of the so-called microgrids, i.e., heterogeneous clusters of DGUs, loads, and storage devices [4], [5].

Manuscript received 16 April 2024; revised 18 June 2024; accepted 13 July 2024. The work of Yu Kawano was supported in part by the Japan Science and Technology Agency (JST) Fusion Oriented Research for Disruptive Science and Technology (FOREST) Program under Grant JPMJFR222E. Recommended by Associate Editor G. Papafotiou. *(Corresponding author: Morteza Nazari Monfared.)*

Morteza Nazari Monfared is with the Department of Electrical, Computer and Biomedical Engineering, University of Pavia, 27100 Pavia, Italy (e-mail: morteza.nazarimonfared01@universitadipavia.it).

Yu Kawano is with the Graduate School of Advance Science and Engineering, Hiroshima University, Higashihiroshima 739-8527, Japan (e-mail: ykawano@hiroshima-u.ac.ip).

Michele Cucuzzella is with the Jan C. Willems Center for Systems and Control, ENTEG, Faculty of Science and Engineering, University of Groningen, 9747 AG Groningen, The Netherlands (e-mail: m.cucuzzella@rug.nl).

Digital Object Identifier 10.1109/TCST.2024.3440228

Although research on microgrids control has primarily focused on alternating current (ac) power networks (see for example [6], [7], [8], [9], [10] and the references therein), the increasing use of RES as DGUs has led to the emergence of direct current (dc) microgrids [11] since many devices such as electric vehicles, electronic devices, batteries, and photovoltaic panels can be directly linked to a dc network, avoiding inefficient conversion stages and also the common frequency and reactive power control issues [12], [13]. Examples of dc microgrid applications encompass modern ships, mobile military bases, trains, airplanes, and electric vehicle charging stations. As a result, interest is growing in dc microgrid control and, specifically, dc–dc power converters (see [14], [15], [16], [17], [18], [19], [20], [21], [22], [23], [24], [25], [26]).

In this article, we investigate a dc–dc boost converter-based dc microgrid, where the main control objective is to regulate the voltage at each node toward a desired level while stabilizing all the other electric signals around the corresponding operating point (see [14], [15], [17], [18], [19], [21], [24], [25], [27], [28], [29], [30]). Moreover, besides achieving voltage regulation, it is crucial for a safe and resilient operation of the overall microgrid that predefined physical constraints are satisfied. More precisely, it is generally required that the voltages evolve in the positive orthant and the duty cycle of each boost converter remains within specified bounds (see [18], [24], [28], [29]). Although saturation mechanisms are a solution to deal with the latter problem, they might deteriorate the closed-loop performance or even lead to instability [31]. Also, the type of information required by the controller is remarkably effective on the system performance. For example, requiring information on the system parameters or time derivatives of the measured electric signals makes the closed-loop system sensitive to uncertainties and noises, affecting the closed-loop performance and stability. In this article, we propose a fully decentralized dynamic control scheme to regulate the voltage of a dc microgrid composed of boost converters supplying unknown loads. We address all the above-mentioned issues and also provide an estimation of the feasible region of attraction for the closed-loop system.

Before explaining in detail the contributions of our work, we first review some of the most important existing results on the control of boost converters.

A. Literature Review

First, we review some of the most important works on control design and stability analysis of a single boost converter;

second we focus our attention on microgrids of boost converters.

A robust passivity-based controller is designed in [14]. However, the voltage positiveness and control signal constraints are not guaranteed and the closed-loop system domain of attraction is not estimated. A proportional-integral (PI) passivity-based controller is designed in [32] to solve the voltage regulation problem for a boost converter connected to a fuel cell. In the case of a known load, global asymptotic stability of the desired equilibrium is guaranteed. Then, to provide robustness with respect to load uncertainty, an Immersion and Invariance parameter estimator is designed together with an adaptive PI passivity-based controller. However, only practical stability can be ensured in this case and the feasibility of the voltage and control signal is not guaranteed (the control signal is limited in simulation by a saturation mechanism). Nonlinear control laws are proposed in [18] and [29] to make the desired equilibrium globally asymptotically stable. However, the constraints on the duty cycles are satisfied by employing a saturation mechanism, the positiveness of the voltage is not analyzed, and information on some system parameters is required. Positiveness of the voltage and constraints on the duty cycle are ensured by the nonlinear controller proposed in [24]. The control design and stability analysis is based on a shifted Lyapunov candidate function and an estimation of the closed-loop system domain of attraction is provided. However, information on the load parameters is required. In [27], a PI-derivative (PID) passivity-based controller is proposed to ensure the global exponential stability of the equilibrium. However, the information on the first-time derivative of the states is required to get satisfactory performance.

Concerning the control design for microgrids of boost converters, in [15], [17], and [30] the design and analysis are based on the linearization of the system around the desired equilibrium point. For example, the controller in [17] is based on sliding mode theory, while the one in [30] is an H_∞ controller based on linear matrix inequalities (LMIs). However, boost converters have a nonlinear dynamic behavior and thus using its linear approximation for control design may deteriorate the closed-loop performance or even lead to instability. Cucuzzella et al. develop a decentralized dynamic controller based on the Krasovskii passivity property of the boost converter (see [33], [34], [35], [36] for more details about Krasovskii passivity). However, no guarantees on the voltage positiveness and duty cycle boundedness are provided and information on the first-time derivative of the states is required, making the control system sensitive to noisy measurements. A plug-and-play (shifted) passivity-based controller is proposed in [28], guaranteeing the asymptotic stability of the desired equilibrium, while satisfying predefined constraints on the duty-cycle through a saturation mechanism. However, the control law for each DGU requires information on the DGU parameters as well as the neighboring line resistances and voltage references.

B. Contribution

Now, the main contributions of our work are listed as follows.

C1: For control design and stability analysis we consider the bilinear dynamics of the boost converter and also the dynamics associated with resistive–inductive power lines. This is a relevant contribution compared with those works that linearize the boost converter dynamics around an equilibrium point (see [15], [17], [30]) and/or neglect the power line dynamics (see [17]).

C2: The proposed controller architecture is fully decentralized and thus scalable, i.e., the controller complexity does not increase with the network size. Indeed, the controller requires only the local measurement of voltage and current and does not need any information on the load parameters or time derivative of the measurements. This is a relevant contribution compared with those controllers that require information on the system parameters (see [18], [24], [27], [28], [29]) and/or time derivative of voltage and current (see [19], [27]), thus improving the robustness against uncertainties and noises.

C3: An estimation of the system's feasible domain of attraction is provided and it is shown that its size depends on the controller gains. This is an essential result to establish the asymptotic stability of the desired equilibrium point and also includes physical constraints.

C4: Compliance with predefined physical constraints, i.e., voltage positiveness and control inputs boundedness, is ensured for any initial condition contained in the estimated feasible domain of attraction. This is a relevant contribution compared with those controllers that do not guarantee that physical constraints are satisfied (see [14], [17]) or employ saturation schemes (see [18], [28], [29], [32]), which might deteriorate the closed-loop performance or even lead to instability [31].

C. Outline

In Section II, the model of a typical dc microgrid is presented and the control problem of interest is formulated. In Section III, an overview of the design and analysis of a dynamic controller for dc microgrids based on differential passivity is provided. Then, the design and analysis of the proposed control scheme is presented. Then, in Section IV, simulation results show the effectiveness of the proposed control system. Finally, some conclusions and possible future research directions are discussed in Section V.

D. Notation

The set of real numbers, nonnegative real numbers, and positive real numbers are denoted by $\mathbb{R}$, $\mathbb{R}_{\geq 0}$, and $\mathbb{R}_{>0}$, respectively. For matrices $A, B \in \mathbb{R}^{n\times m}$, we write $A \leq B$ ($A < B$) if and only if $A_{i,j} \leq B_{i,j}$ ($A_{i,j} < B_{i,j}$) for all $i = 1, \ldots, n$ and $j = 1, \ldots, m$, where $A_{i,j}$ denotes the (i, j)th component of A. The n-dimensional vector whose all components are 1 is denoted by $\mathbb{1}_n$. For two given vectors $x, y \in \mathbb{R}^n$, the Hadamard product, denoted by $(x \circ y) \in \mathbb{R}^n$, is a vector with elements $(x \circ y)_j = x_j y_j$ for $j = 1, \ldots, n$. Given a vector $x \in \mathbb{R}^n$, $[x] \in \mathbb{R}^{n\times n}$ denotes the diagonal matrix whose diagonal entries are the components of x. The Euclidean norm

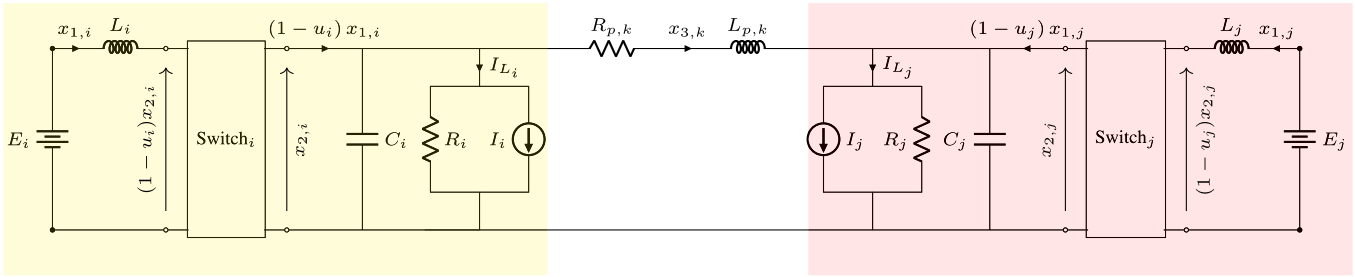

Fig. 1. Electrical scheme of nodes (DGUs) i and j interconnected through a power line k.

of a vector $x \in \mathbb{R}^q$ weighted by a matrix $Q \in \mathbb{R}^{q\times q}$ is denoted by $\|x\|_Q := (x^\top Q x)^{1/2}$. Given $x \in \mathbb{R}^n$, $y \in \mathbb{R}^m$, we compactly denote $(x, y) = (x^\top, y^\top)^\top$.

II. Preliminaries

This article focuses on a typical dc microgrid composed of n DGUs supplying local loads and interconnected with each other through m transmission power lines. First, for the reader's convenience, a brief introduction to the considered dc microgrid along with its dynamics is presented. Then, we formulate the control problem we solve in this work.

A. DC Microgrid Modeling

The dc network is represented by a connected and (ordered) undirected graph $\mathcal{G} = (\mathcal{V}, \mathcal{E})$, where $\mathcal{V} = \{1, \dots, n\}$ and $\mathcal{E} = \{1, \dots, m\}$ indicate the nodes and edges set. Each node $i \in \mathcal{V}$ represents a DGU consisting of a dc–dc boost converter supplying a local load. Nodes are interconnected with each other through resistive–inductive power lines and the topology of the network is described by the incidence matrix D associated with $\mathcal{G}$. Fig. 1 shows the schematic electrical diagram of two nodes interconnected through a power line k.

Each boost converter includes a voltage source E_i, an inductor L_i, and a capacitor C_i. The current through the inductor and the voltage across the capacitor are denoted by $x_{1,i}(t)$ and $x_{2,i}(t)$, respectively. Each load absorbs a current denoted by $I_{L_i}(x_{2,i})$ and consists of the parallel combination of a resistor R_i and a constant current I_i, i.e., $I_{L_i}(x_{2,i}) = I_i + R_i^{-1}x_{2,i}$. Moreover, the current through the inductor $L_{p,k}$ of the kth power line, with $k \in \mathcal{E}$, is denoted by $x_{3,k}(t)$, while the resistance $R_{p,k}$ captures the distribution power losses.

By employing each boost converter with the pulse width modulation (PWM) technique with a sufficiently high frequency, the switching dynamics of each converter can be approximated by its average behavior. Then, by applying the Kirchhoff's laws, the average dynamics of the node i can be written as

$$L_i \dot{x}_{1,i} = -(1-u_i)\,x_{2,i} + E_i \tag{1a}$$
$$C_i \dot{x}_{2,i} = (1-u_i)\,x_{1,i} - I_i - R_i^{-1}x_{2,i} - x_{3,k} \tag{1b}$$
$$L_{p,k}\dot{x}_{3,k} = \left(x_{2,i} - x_{2_j}\right) - R_{p,k}x_{3,k} \tag{1c}$$

where u_i denotes the so-called duty cycle of the converter and satisfies $u_i(t) \in [0, 1]$ for all $i \in \mathcal{V}$ (see [37] for more details). Then, system (1) can be written compactly for all nodes $i \in \mathcal{V}$ as follows [19]:

$$L\dot{x}_1 = -(\mathbb{1}_n - u) \circ x_2 + E \tag{2a}$$
$$C\dot{x}_2 = (\mathbb{1}_n - u) \circ x_1 - I - R^{-1}x_2 + Dx_3 \tag{2b}$$
$$L_p\dot{x}_3 = -D^\top x_2 - R_p x_3 \tag{2c}$$

where $x_1 : \mathbb{R}_{\geq 0} \to \mathbb{R}^n$, $x_2 : \mathbb{R}_{\geq 0} \to \mathbb{R}^n_{>0}$, $u : \mathbb{R}_{\geq 0} \to [0, 1]^n$ denote the node current, voltage, and control input vectors, respectively. The vector of the currents through the power lines is denoted by $x_3 : \mathbb{R}_{\geq 0} \to \mathbb{R}^m$. Also, $x := (x_1^\top, x_2^\top, x_3^\top)^\top$ denotes the system state vector. The matrices $L, C \in \mathbb{R}^{n\times n}_{>0}$ and $R_p, L_p \in \mathbb{R}^{m\times m}_{>0}$ are diagonal with entries equal to the corresponding values of the ith DGU or kth power line. The vector $E = (E_1, \dots, E_n)^\top$ denotes the voltage sources, while the load parameters are denoted by the vector $I = (I_1, \dots, I_n)^\top$ and the diagonal matrix R, with both I and R unknown.

The incidence matrix $D \in \mathbb{R}^{n\times m}$ represents the topology of the considered dc microgrid, where the ends of each edge k are arbitrarily labeled with positive or negative signs. More precisely, $D_{ik} = 1$ if i is the positive end of k, $D_{ik} = -1$ if i is the negative end of k, and $D_{ik} = 0$ otherwise. Now, we are ready to formulate the control problem we solve in this article.

B. Problem Formulation

In this article, we focus on regulating the network voltage toward a desired reference while satisfying physical constraints. Before formulating the control problem, we first show that given a desired voltage reference $x_2^* \geq E \in \mathbb{R}^n_{>0}$, the equilibrium (x^*, u^*) of (2) is uniquely determined by

$$x_1^* = [E]^{-1}\left[x_2^*\right]\left(I + R^{-1}x_2^* + DR_p^{-1}D^\top x_2^*\right) \tag{3a}$$
$$x_3^* = -R_p^{-1}D^\top x_2^* \tag{3b}$$
$$u^* = \mathbb{1}_n - \left[x_2^*\right]^{-1}E. \tag{3c}$$

The value of the desired voltage x_2^* is usually selected in accordance with standards, and operational requirements, and to ensure optimal performance and safety of the electrical equipment (e.g., loads). Alternatively, it might be generated by a higher-level control scheme by solving an optimization problem aiming to guarantee optimal operation and efficiency of the overall network (e.g., load sharing). In order to explain the rationale of the control design approach that we propose in Section III, it is worth emphasizing that the relation between

u^* and x_2^* in (3c) does not require any information of the topology of the network and load parameters.

Remark 1: From (3c), $x_2^* \geq E \in \mathbb{R}^n_{>0}$ if and only if $u^* \in [0,1)^n$, which implies that there are one-to-one correspondences among u^*, x_2^*, and (x^*, u^*). $\lhd$

Then, as natural physical constraints, we require $x_2(\cdot) \in \mathbb{R}^n_{>0}$ and $u(\cdot) \in [0,1]^n$. The first constraint implies that the voltages evolve in the positive orthant for all the time, while the second one is required to guarantee the proper functioning of each boost converter.

Now, we are ready to formulate the voltage regulation problem for the considered dc microgrid (2).

Problem 1: Given a desired voltage reference $x_2^* \geq E \in \mathbb{R}^n_{>0}$, stabilize the dc microgrid (2) at the equilibrium point (x^*, u^*) given by (3), while satisfying the physical constraints $x_2(t) \in \mathbb{R}^n_{>0}$ and $u(t) \in [0,1]^n$ for all $t \geq 0$. $\lhd$

Note that the simplest stabilizing controller is given by $u = u^*$. However, it does not provide any possibility to improve transient performance as will be shown through simulations in Section IV. This is the main reason that motivates us to design in Section III a dynamic feedback controller solving Problem 1, which is, to the best of our knowledge, a relevant contribution to the existing literature. For example, in [17], the authors design a robust decentralized control scheme based on a second-order sliding mode, guaranteeing convergence to the desired voltage despite the presence of model and load parameter uncertainties. However, only local stability is ensured, physical constraints are not guaranteed and an estimate of the region of attraction is not provided. In [28], a shifted passivity-based control scheme is designed to ensure global stability. However, each controller requires information on the desired equilibrium point, i.e., load parameters and resistance of the power lines interconnecting neighboring nodes. The controller proposed in [19] is based on Krasovskii passivity and thus the control scheme does not require any information on either load parameters or resistance of the power lines. However, the control law employs both current and voltage time derivatives, which might deteriorate the closed-loop performance in the presence of noisy measurements.

In the next section, we design a novel decentralized voltage control scheme that solves Problem 1 without using any information on the load parameters, power line resistances, and time derivative of current and voltage.

III. Main Results

In this section, we provide a dynamic stabilizing state-feedback controller for the considered dc microgrid (2), addressing the drawback of the shifted and Krasovskii passivity based controllers proposed in [19] and [28], respectively, which require information of the load and other system parameters or time-derivatives of the state variables. The proposed controller instead can be implemented by using information only about the voltage source. To design such a controller, we revisit the results in [19] from the perspective of differential passivity [38], [39]. Then, we reveal that the drawback of the controller proposed in [19] is caused by the integrability issue of differential-passivity-based control. In this article we solve this issue and, additionally, we characterize the set of initial states ensuring that the corresponding closed-loop trajectories fulfill predefined physical constraints.

A. Differential Passivity Analysis

We introduce now the notion of a variational system, which is instrumental to analyzing later the differential passivity property of the considered dc network (2).

Consider the nonlinear system

$$\dot{x} = f(x,u) \tag{4}$$

where $x : \mathbb{R}_{\geq 0} \to \mathbb{R}^n$ and $u : \mathbb{R}_{\geq 0} \to \mathbb{R}^m$ are, respectively, the state variables and control input vectors. The notion of differential passivity is investigated for the so-called "prolonged system" (see [38]), which comprises the nonlinear system (4) and the associated variational system along the trajectory $(x(t), u(t))$, i.e.,

$$\dot{\delta x} = \frac{\partial f(x,u)}{\partial x}\delta x + \frac{\partial f(x,u)}{\partial u}\delta u \tag{5}$$

where $\delta x : \mathbb{R}_{\geq 0} \to \mathbb{R}^n$ and $\delta u : \mathbb{R}_{\geq 0} \to \mathbb{R}^m$ represent, respectively, the state variable and control input vectors of the variational system [34]. More precisely, δx and δu denote infinitesimal variations of (x,u) with respect to neighboring solutions [40]. Now, we can analyze the differential passivity property of the dc network (2).

To analyze the differential passivity of the dc network (2), we consider its variational system, i.e.,

$$L\dot{\delta x}_1 = \delta u \circ x_2 - (\mathbb{1}_n - u) \circ \delta x_2 \tag{6a}$$

$$C\dot{\delta x}_2 = -\delta u \circ x_1 + (\mathbb{1}_n - u) \circ \delta x_1 - R^{-1}\delta x_2 + D\delta x_3 \tag{6b}$$

$$L_p\dot{\delta x}_3 = -D^\top \delta x_2 - R_p \delta x_3 \tag{6c}$$

with the state $(\delta x_1, \delta x_2, \delta x_3) \in \mathbb{R}^n \times \mathbb{R}^n \times \mathbb{R}^m$ and input $\delta u \in \mathbb{R}^n$.

System (6) is passive in the following sense.

Theorem 1: Consider a dc network (2) and its variational system (6). Then, the variational system is passive with respect to the supply rate $\delta u^\top(\delta x_1 \circ x_2 - x_1 \circ \delta x_2)$ and the storage function

$$S(x,\delta x) = \frac{1}{2}\left(\|\delta x_1\|_L^2 + \|\delta x_2\|_C^2 + \|\delta x_3\|_{L_p}^2\right) \tag{7}$$

for all $(x,u), (\delta x, \delta u) \in (\mathbb{R}^n \times \mathbb{R}^n \times \mathbb{R}^m) \times \mathbb{R}^n$.

Proof: The storage function (7) satisfies

$$\begin{aligned}\dot{S}(x,\delta x) &= \delta x_1^\top L\dot{\delta x}_1 + \delta x_2^\top C\dot{\delta x}_2 + \delta x_3^\top L_p \dot{\delta x}_3 \\ &= \delta u^\top(\delta x_1 \circ x_2 - x_1 \circ \delta x_2) \\ &\quad - \|\delta x_2\|_{R^{-1}}^2 - \|\delta x_3\|_{R_p}^2\end{aligned}$$

along the solutions of (6), which completes the proof. ■

The above passivity property is called differential passivity. As for standard passivity, one may expect a differential passivity-based controller for stabilization of the following form:

$$\delta u = -K_1(\delta x_1 \circ x_2 - x_1 \circ \delta x_2) \tag{8}$$

where $K_1 \in \mathbb{R}^{n\times n}$ is a diagonal and positive definite matrix with entries $k_{1,i}, i = 1, \ldots, n$. However, since $\delta x_1 \circ x_2 - x_1 \circ \delta x_2$ is not integrable, this is not directly helpful to design a stabilizing controller for a dc network (2).

To address this issue, the concept of Krasovskii passivity [34] has been introduced based on the fact that $(\delta x, \delta u) = (\dot{x}, \dot{u})$ satisfies the dynamics of the variational system (6). This yields the following dynamic controller [19], [33]:

$$\dot{u} = -K_1(\dot{x}_1 \circ x_2 - x_1 \circ \dot{x}_2).$$

Moreover, based on the input shaping technique proposed in [33], in order to specify the input reference u^*, the above controller can be modified as follows:

$$\dot{u} = K_2(u^* - u) - K_1(\dot{x}_1 \circ x_2 - x_1 \circ \dot{x}_2) \tag{9}$$

where $K_2 \in \mathbb{R}^{n\times n}$ is a diagonal and positive definite matrix with entries $k_{2,i}, i = 1, \ldots, n$. In fact, asymptotic stability of the closed-loop system at (x^*, u^*) is shown by utilizing the following Krasovskii Lyapunov function [19], [33]:

$$V(\dot{x}, u) := \frac{1}{2}\Big(\|\dot{x}_1\|_L^2 + \|\dot{x}_2\|_C^2 + \|\dot{x}_3\|_{L_p}^2 + \|u - u^*\|_{K_2K_1^{-1}}^2\Big). \tag{10}$$

However, neither in [19] nor in [33] guarantees are provided on compliance with predefined physical constraints. Furthermore, the controller (9) requires information on the time-derivatives of the current x_1 and voltage x_2 of all nodes, which can deteriorate the closed-loop performance in the case of noisy measurements.

B. Dynamic Control Design

We first solve the integrability issue of the differential passivity-based controller (8) by rewriting it in the following decentralized way:

$$\delta u_i = -k_{1,i}(x_{2,i}\delta x_{1,i} - x_{1,i}\delta x_{2,i}), \quad i = 1, \ldots, n. \tag{11}$$

Then, the right-hand side of (11) can be made integrable by multiplying it by the integrating factor $1/x_{1,i}x_{2,i}$. Based on this, a static stabilizing controller is presented by [24]. However, its implementation requires information of x_1^*, i.e., of system parameters E, I, R, R_p, and D. Some of their values are not easy to know in practice. To address this problem, we modify each component of the Krasovskii passivity-based controller (9) as follows:

$$\dot{u}_i = \frac{1}{x_{1,i}x_{2,i}}\left(k_{2,i}\left(u_i^* - u_i\right) - k_{1,i}\left(\dot{x}_{1,i}x_{2,i} - x_{1,i}\dot{x}_{2,i}\right)\right)$$

which can be rewritten as

$$u_i = k_{1,i}\ln(x_{2,i}/x_{1,i}) + v_i$$
$$\dot{v}_i = k_{2,i}\left(u_i^* - u_i\right) / \left(x_{1,i}x_{2,i}\right)$$

with $k_{2,i} > 0$. The only system parameter required for its implementation is u^*, i.e., the source voltage E. However, since $x_{2,i} > 0$, u_i is not defined when $x_{1,i} \le 0$.

To deal with this issue, we employ a switching structure for u_i leading to the following dynamic state-feedback controller:

$$u_i = \begin{cases} \operatorname{sign}(x_{1,i})\left(k_{1,i}\ln\left(\left|x_{2,i}x_{1,i}^{-1}\right|\right) + v_i\right); & \text{if } |x_{1,i}| > \varepsilon_i \\ u_i^*; & \text{if } |x_{1,i}| \le \varepsilon_i \end{cases} \tag{12a}$$

$$\dot{v}_i = k_{2,i}\left(u_i^* - u_i\right) / \left(x_{1,i}x_{2,i}\right) \tag{12b}$$

where $v_i \in \mathbb{R}$ is the state of the controller dynamics, $k_{1,i}, k_{2,i} \in \mathbb{R}_{>0}$ are tuning parameters, and $\varepsilon_i \in \mathbb{R}_{>0}$ is the threshold that specifies the switching condition. For the sake of closed-loop analysis, we define $k_1 := (k_{1,1}, \ldots, k_{1,n})^\top$, $k_2 := (k_{2,1}, \ldots, k_{2,n})^\top$, and $\varepsilon := (\varepsilon_1, \ldots, \varepsilon_n)^\top$.

It is worth emphasizing that the dynamic controller (12) is fully decentralized, i.e., each control input u_i can be computed by measuring only the local value of the current $x_{1,i}$ and voltage $x_{2,i}$ of node i. Also, $u_i^* = 1 - E_i/x_{2,i}^*$ depends only on the local voltage source and reference.

As the main contribution of this article, we show that the fully decentralized controller (12) asymptotically stabilizes the equilibrium point of the closed-loop system. Moreover, we estimate a region of attraction, which can be utilized to characterize the set of initial states such that the corresponding closed-loop trajectories fulfill predefined psychical constraints.

Theorem 2: Given $x_2^* \ge E \in \mathbb{R}_{>0}^n$, consider the closed-loop system consisting of a dc microgrid (2) and the decentralized controller (12). Also, let Ω_c denote the level set of the Krasovskii Lyapunov function (10), i.e.,

$$\Omega_c := \left\{(x, u) \in \left(\mathbb{R}^n \times \mathbb{R}^n \times \mathbb{R}^m\right) \times \mathbb{R}^n : V(\dot{x}, u) \le c\right\}. \tag{13}$$

Then, the following statements hold:

1) for any $k_1, k_2, \varepsilon \in \mathbb{R}_{>0}^n$, the closed-loop system is asymptotically stable at (x^*, u^*);
2) if Ω_c is contained in $(\mathbb{R}^n \times \mathbb{R}_{>0}^n \times \mathbb{R}^m) \times [0, 1)^n$, then Ω_c is a region of attraction;
3) Ω_c is contained in $(\mathbb{R}^n \times \mathbb{R}_{>0}^n \times \mathbb{R}^m) \times [0, 1)^n$ if and only if

$$c \le \min_{i\in\mathcal{V}}\left\{\frac{k_{2,i}}{2k_{1,i}}\left(u_i^*\right)^2\right\}, \quad c < \min_{i\in\mathcal{V}}\left\{\frac{E_i^2}{2L_i}\right\}. \tag{14}$$

Proof:

Proof of Items 1) and 2): Let $\bar{V}(x, u)$ be the function obtained by substituting $\dot{x}$ given by (2) into the Krasovskii Lyapunov function $V(\dot{x}, u)$ in (10). Then, we have

$$\begin{aligned}\bar{V}(x, u) &= \frac{1}{2}\Big(\|-(\mathbb{1}_n - u)\circ x_2 + E\|_{L^{-1}}^2 \\ &\quad + \|(\mathbb{1}_n - u)\circ x_1 - I - R^{-1}x_2 + Dx_3\|_{C^{-1}}^2 \\ &\quad + \|D^\top x_2 + R_p x_3\|_{L_p^{-1}}^2 + \|u - u^*\|_{K_2K_1^{-1}}^2\Big).\end{aligned} \tag{15}$$

By Remark 1, $\bar{V}(x, u)$ in (15), or equivalently $V(\dot{x}, u)$ in (10), is positive definite at (x^*, u^*) on $(\mathbb{R}^n \times \mathbb{R}^n \times \mathbb{R}^m) \times [0, 1)^n$.

Thus, stability can be shown by taking the time-derivative of $\bar{V}(x, u)$, or equivalently $V(\dot{x}, u)$, along the closed-loop

trajectory. To this end, we calculate the time derivative of (2) yielding

$$L\ddot{x}_1 = -\left(\mathbb{1}_n - u\right) \circ \dot{x}_2 + \dot{u} \circ x_2 \tag{16a}$$
$$C\ddot{x}_2 = \left(\mathbb{1}_n - u\right) \circ \dot{x}_1 - \dot{u} \circ x_1 - R^{-1}\dot{x}_2 + D\dot{x}_3 \tag{16b}$$
$$L_p\ddot{x}_3 = -D^\top \dot{x}_2 - R_p\dot{x}_3. \tag{16c}$$

Also, from the controller (12), we have

$$\dot{u}_i = \begin{cases} -\dfrac{k_{1,i}\operatorname{sign}\left(x_{1,i}\right)}{x_{1,i}x_{2,i}}\Big(\dot{x}_{1,i}x_{2,i} - x_{1,i}\dot{x}_{2,i} \\ \qquad + k_{1,i}^{-1}k_{2,i}\left(u_i - u_i^*\right)\Big); & \text{if } \left|x_{1,i}\right| > \varepsilon_i \\ 0; & \text{if } \left|x_{1,i}\right| \le \varepsilon_i. \end{cases} \tag{17}$$

By using (16), the time-derivative of $V(\dot{x}, u)$ along the closed-loop trajectory is computed as

$$\begin{aligned} &\dot{V}\left(\dot{x}, u\right) \\ &= \dot{x}_1^\top L\ddot{x}_1 + \dot{x}_2^\top C\ddot{x}_2 + \dot{x}_3^\top L_p\ddot{x}_3 + \left(u - u^*\right)^\top K_2K_1^{-1}\dot{u} \\ &= \dot{x}_1^\top\left(x_2 \circ \dot{u}\right) - \dot{x}_2^\top\left(x_1 \circ \dot{u}\right) + \left(u - u^*\right)^\top K_2K_1^{-1}\dot{u} \\ &\quad - \dot{x}_2^\top R^{-1}\dot{x}_2 - \dot{x}_3^\top R_p\dot{x}_3 \\ &= \dot{u}^\top\left(\dot{x}_1 \circ x_2 - x_1 \circ \dot{x}_2 + K_2K_1^{-1}\left(u - u^*\right)\right) \\ &\quad - \dot{x}_2^\top R^{-1}\dot{x}_2 - \dot{x}_3^\top R_p\dot{x}_3 \end{aligned}$$

where note that $K_2K_1^{-1}$ is a diagonal matrix. By rewriting the first term of the last equation element-wisely, we obtain

$$\begin{aligned} \dot{V}\left(\dot{x}, u\right) = &\sum_{i=1}^{n}\left(\dot{u}_i\left(\dot{x}_{1,i}x_{2,i} - x_{1,i}\dot{x}_{2,i} + k_{2,i}k_{1,i}^{-1}\left(u_i - u_i^*\right)\right)\right) \\ &- \dot{x}_2^\top R^{-1}\dot{x}_2 - \dot{x}_3^\top R_p\dot{x}_3. \end{aligned} \tag{18}$$

Without loss of generality, we suppose that $x_{1,i} > \varepsilon_i$ for $i = 1, \ldots, h$, $x_{1,j} < -\varepsilon_j$ for $j = h+1, \ldots, q$, and $|x_{1,l}| \le \varepsilon_l$ for $l = q+1, \ldots, n$. Then, it follows from (17) and (18) that:

$$\begin{aligned} \dot{V}\left(\dot{x}, u\right) &= -\sum_{i=1}^{h}k_{1,i}^{-1}x_{1,i}x_{2,i}\dot{u}_i^2 + \sum_{j=h+1}^{q}k_{1,j}^{-1}x_{1,j}x_{2,j}\dot{u}_j^2 \\ &\quad - \dot{x}_2^\top R^{-1}\dot{x}_2 - \dot{x}_3^\top R_p\dot{x}_3 \\ &< -\sum_{i=1}^{q}k_{1,i}^{-1}\varepsilon_i x_{2,i}\dot{u}_i^2 - \dot{x}_2^\top R^{-1}\dot{x}_2 - \dot{x}_3^\top R_p\dot{x}_3. \end{aligned} \tag{19}$$

Thus, $\dot{V}(\dot{x}, u)$ (equivalently $\dot{\bar{V}}(x, u)$) is negative semi-definite at (x^*, u^*) if $x_2 \in \mathbb{R}^n_{>0}$.

In summary, $V(\dot{x}, u)$ and $\dot{V}(\dot{x}, u)$ are, respectively, positive definite and negative semi-definite at (x^*, u^*) on $(\mathbb{R}^n \times \mathbb{R}^n_{>0} \times \mathbb{R}^m) \times [0, 1)^n$. Therefore, (x^*, u^*) is stable by the Lyapunov stability theorem. Next, we show the asymptotic stability of (x^*, u^*) by invoking LaSalle's invariance principle [41, Theorem 4.4].

Consider a level set Ω_c of $V(\dot{x}, u)$ given by (13) and let $c > 0$ be such that $\Omega_c \subset (\mathbb{R}^n \times \mathbb{R}^n_{>0} \times \mathbb{R}^m) \times [0, 1)^n$. From $V(\dot{x}, u) = \bar{V}(x, u)$ and (15), Ω_c is compact because of $u < \mathbb{1}_n$. Also, from the above discussion, Ω_c is positively invariant.

Define $\Upsilon := \Upsilon_{|x_1|>\varepsilon} \cup \Upsilon_{|x_1|\le\varepsilon}$, where

$$\Upsilon_{|x_1|>\varepsilon} := \left\{(x, u) \in \Omega_c : |x_1| > \varepsilon, \dot{V}\left(\dot{x}, u\right) = 0\right\}$$
$$\Upsilon_{|x_1|\le\varepsilon} := \left\{(x, u) \in \Omega_c : |x_1| \le \varepsilon, \dot{V}\left(\dot{x}, u\right) = 0\right\}.$$

Recall that R and R_p are symmetric and positive definite matrices. From (19) with $x_2 \in \mathbb{R}^n_{>0}$ on Ω_c, we have

$$\begin{aligned} \Upsilon_{|x_1|>\varepsilon} = \{(x, u) \in \Omega_c : \ &|x_1| > \varepsilon, \dot{x}_2 = 0, \dot{x}_3 = 0 \\ &\dot{u}_i = 0, i = 1, \ldots, q\}. \end{aligned} \tag{20}$$

Also, from (12a) and (19), we obtain

$$\begin{aligned} \Upsilon_{|x_1|\le\varepsilon} = \{(x, u) \in \Omega_c : \ &|x_1| \le \varepsilon, \dot{x}_2 = 0, \dot{x}_3 = 0 \\ &u_i = u_i^*, i = q+1, \ldots, n\}. \end{aligned} \tag{21}$$

Let Φ be the largest invariant set contained in Υ. This is contained in $\Upsilon \cap \{(x, u) \in \Omega_c : \ddot{x}_2 = 0\}$. From (16b), (20), (21), and $u \ne \mathbb{1}_n$ on Υ, we have

$$\begin{aligned} \Phi &\subset \Upsilon \cap \{(x, u) \in \Omega_c : \ddot{x}_2 = 0\} \\ &= \Upsilon \cap \{(x, u) \in \Omega_c : \dot{x}_1 = 0\} \\ &= \{(x, u) \in \Omega_c : |x_1| > \varepsilon, \dot{x} = 0, \dot{u}_i = 0, i = 1, \ldots, q\} \\ &\quad \cup \{(x, u) \in \Omega_c : |x_1| \le \varepsilon, \dot{x} = 0, \\ &\qquad u_i = u_i^*, i = q+1, \ldots, n\}. \end{aligned}$$

Moreover, (17) and (20) imply

$$\begin{aligned} &\{(x, u) \in \Omega_c : |x_1| > \varepsilon, \dot{x} = 0, \dot{u}_i = 0, i = 1, \ldots, q\} \\ &\quad = \{(x, u) \in \Omega_c : |x_1| > \varepsilon, \dot{x} = 0, u_i = u_i^*, i = 1, \ldots, q\}. \end{aligned}$$

Therefore, we have

$$\Phi \subset \{(x, u) \in \Omega_c : \dot{x} = 0, u = u^*\}$$

and consequently, from Remark 1

$$\{(x, u) \in \Omega_c : \dot{x} = 0, u = u^*\} = \{(x^*, u^*)\}.$$

Thus, the closed-loop systems is asymptotically stable at (x^*, u^*), and the region of attraction contains Ω_c.

Proof of Item 3): The idea behind the proof of this item origins from geometric considerations. Specifically, the aim is to obtain the tightest level set Ω_c that is contained in the region bounded by the lines $x_{2,i} = 0$, $u_i = 1$, and $u_i = 0$, without crossing the lines $x_{2,i} = 0$ and $u_i = 1$, for all $i \in \mathcal{V}$.

Noting that $V(\dot{x}, u) = \bar{V}(x, u)$, we use $\bar{V}(x, u)$ in (15). First, let $\Omega_{c_{x_{2,0,i}}}$ denote the level set whose border is tangent to the line $x_{2,i} = 0$. This means that $\Omega_{c_{x_{2,0,i}}}$ is the tightest level set that is contained in the region bounded by the line $x_{2,i} = 0$ and does not cross such a line if and only if $c < c_{x_{2,0,i}}$ for all $i \in \mathcal{V}$. Then, the set $\Omega_{c_{x_{2,0,i}}}$ is tangent to the line $x_{2,i} = 0$ if and only if

$$c_{x_{2,0,i}} = \frac{E_i^2}{2L_i}$$

which is obtained by substituting $x_{2,i} = 0$ in (15) and considering the quadratic form of $\bar{V}(x, u)$, i.e.,

$$c_{x_{2,0,i}} = \min_{x_1, x_2, x_3, u}\left\{\bar{V}(x, u)|_{x_{2,i}=0}\right\} = \frac{E_i^2}{2L_i}.$$

Next, by repeating similar steps as above, the level set $\Omega_{c_{u,0,i}}$ is tangent to the line $u_i = 0$ if and only if

$$c_{u,0,i} = \frac{k_{2,i}}{2k_{1,i}}\left(u_i^*\right)^2.$$

Finally, the level set $\Omega_{c_{u,1,i}}$ is tangent to the line $u_i = 1$ if and only if

$$c_{u,1,i} = \frac{E_i^2}{2L_i} + \frac{k_{2,i}}{2k_{1,i}}\left(1 - u_i^*\right)^2.$$

Therefore, $\Omega_c \subset (\mathbb{R}^n \times \mathbb{R}^n_{>0} \times \mathbb{R}^m) \times [0,1)^n$ if and only if the following inequalities are satisfied:

$$c \leq \min_{i\in\mathcal{V}} \left\{ \frac{k_{2,i}}{2k_{1,i}}\left(u_i^*\right)^2 \right\}$$
$$c < \min_{i\in\mathcal{V}} \left\{ \frac{E_i^2}{2L_i}, \frac{E_i^2}{2L_i} + \frac{k_{2,i}}{2k_{1,i}}\left(1 - u_i^*\right)^2 \right\} = \min_{i\in\mathcal{V}} \left\{ \frac{E_i^2}{2L_i} \right\}$$

i.e., (14) holds. ■

Remark 2: Although (12) is a switching controller, (10) is used as a common Lyapunov function for both controllers. Therefore, we can guarantee the closed-loop stability. ◁

Remark 3: According to Theorem 2, any closed-loop trajectory starting from Ω_c converges to (x^*, u^*) while fulfilling the physical constraints $x_2(\cdot) \in \mathbb{R}^n_{>0}$ and $u(\cdot) \in [0,1]^n$ if c satisfies (14). Thus, we call Ω_c with c satisfying (14) a feasible region of attraction. From (14) and (15), it is evident that the size of the feasible region of attraction Ω_c depends on the ratio of the tuning parameters, i.e., $k_{2,i}/k_{1,i}$. Since c is upperbounded by $E_i^2/2L_i$ [see (14)], then the largest feasible region of attraction Ω_c is obtained when $k_{1,i}$ and $k_{2,i}$ are selected as

$$\frac{k_{2,i}}{k_{1,i}} \geq \frac{E_i^2}{L_i\left(1 - E_i/x_{2,i}^*\right)^2}, \quad i = 1, \ldots, n \tag{22}$$

which follows from imposing $(k_{2,i}/2k_{1,i})(u_i^*)^2 \geq (E_i^2/2L_i)$ and using (3c). In this case, Ω_{c_l} is a feasible region of attraction for

$$c_l = \min_{i\in\mathcal{V}} \left\{ \frac{E_i^2}{2L_i} \right\} - \varepsilon_l \tag{23}$$

where $\varepsilon_l > 0$ is allowed to be arbitrarily small. ◁

Now, in the following corollary, we extend the results of Theorem 2 to the case of dc networks including the so-called ZIP loads, i.e., nonlinear loads consisting of the parallel combination of constant impedance (Z), current (I), and power (P) components. Therefore, we consider now also constant power loads (CPLs) in addition to the constant resistance and current (ZI) loads considered in Theorem 2. The current–voltage characteristic of such loads is given by $I_L(x_2) = R^{-1}x_2 + I + [x_2]^{-1}P$, where $P = \left(P_1, \ldots, P_n\right)^\top$ and P_i denotes the constant power absorbed by the CPL of node i (see [19]). Before introducing the corollary, it is noteworthy to emphasize that the structure of the controller in (12) remains unchanged. Also, let us define the set $\mathcal{R}$ as

$$\mathcal{R} = \left\{ x_{2,i} \in \mathbb{R}_{>0} : x_{2,i} > \sqrt{\beta_{1,i}\beta_{2,i}},\ i \in \mathcal{V} \right\} \tag{24}$$

where $0 \leq P_i \leq \beta_{1,i}$ and $0 \leq R_i \leq \beta_{2,i}$, with $\beta_{1,i}$ and $\beta_{2,i}$ being known positive constants for all $i \in \mathcal{V}$.

Corollary 1: Given $E \leq x_2^* \in \mathcal{R}^n$, consider a dc microgrid (2) with ZIP loads and in closed-loop with the controller (12). Then, the equilibrium point (x^*, u^*) is asymptotically stable with an estimated feasible region of attraction Ω_c that is contained in $(\mathbb{R}^n \times \mathcal{R}^n \times \mathbb{R}^m) \times [0,1)^n$. Furthermore, Ω_c is contained in $(\mathbb{R}^n \times \mathcal{R}^n \times \mathbb{R}^m) \times [0,1)^n$ if and only if

$$c \leq \min_{i\in\mathcal{V}} \left\{ \frac{k_{2,i}}{2k_{1,i}}\left(u_i^*\right)^2 \right\} \tag{25a}$$

$$c < \min_{i\in\mathcal{V}} \left\{ \frac{\left(E_i - \left(1 - u_i^*\right)\sqrt{\beta_{1,i}\beta_{2,i}}\right)^2}{2L_i} \right\}. \tag{25b}$$

Proof: The proof is given in the Appendix. ■

Theorem 2 guarantees asymptotic stability of the desired equilibrium for any positive value of the controller gains $k_{1,i}$ and $k_{2,i}$. However, we provide in the following remark some insights for a finer tuning of these gains.

Remark 4: A careful inspection of $\dot{u}$ in (17) reveals that larger values of k_2 result in a faster convergence of u toward its desired value u^*. Second, from (19), it follows that the convergence rate of $V(\dot{x}, u)$ toward zero is influenced by k_1. Specifically, a smaller value for k_1 increases the convergence speed of $V(\dot{x}, u)$ toward zero and, therefore, the convergence to the desired equilibrium point. Given these general tuning considerations, for the specific values of k_1 and k_2, a trial and error procedure can be adopted based on the specific requirements of the considered dc network. Furthermore, it is worth noticing that the ratio $k_{2,i}/k_{1,i}$ influences the shape and size of the estimated feasible region of attraction, as outlined in (14), (22), and (23). Therefore, obtaining the largest estimation of the feasible region of attraction requires choosing k_1 and k_2 satisfying (22). Finally, we emphasize that the controller gains for each node can be tuned independently of each other. ◁

IV. Simulations

In this section, in order to validate the theoretical results discussed in Section III, we test in simulation the proposed control scheme (12). First, in order to provide a better understanding of our analysis we consider the single-node and two-node cases (see [17], [19], [42]). Then, we simulate a more realistic dc network with four nodes in ring topology, including ZIP loads.

A. Single-Node Case

In this section, we focus on a single boost converter by selecting $n = 1$ and $m = 0$ in (2). Namely, we consider the system

$$\begin{aligned} L\dot{x}_1 &= -(1-u)\,x_2 + E \\ C\dot{x}_2 &= (1-u)\,x_1 - I - x_2/R \end{aligned} \tag{26}$$

where each parameter and the desired voltage reference are taken from a real microgrid (see [17], [19], [42]) and are reported in Table I. We first validate items 1)–3) of Theorem 2.

TABLE I
VALUES OF THE SYSTEM PARAMETERS

Parameter	Value	Parameter	Value
L	0.00112 (H)	C	0.0068 (F)
E	280 (V)	I	50 (A)
R	10 (Ω)	x_2^*	380 (V)
R_p	39×10^{-3} (Ω)	L_p	86×10^{-6} (H)

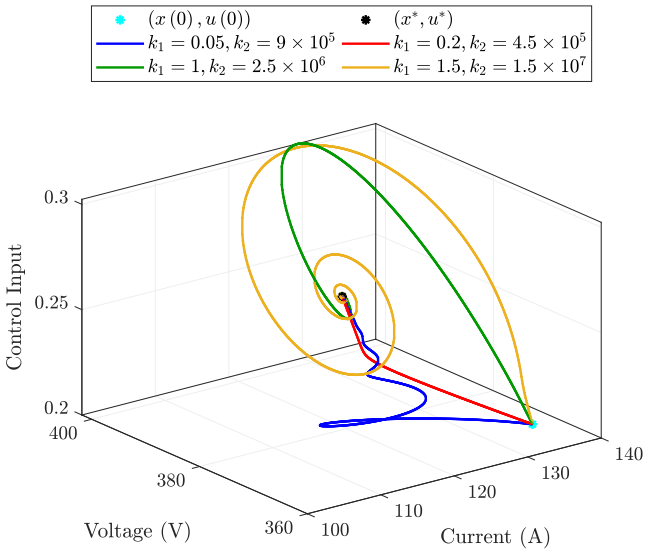

Fig. 2. Closed-loop trajectories for four different pairs of the controller gains k_1, k_2.

Then, we observe the effects of the switching mechanism employed in (12). Finally, we compare the proposed dynamic controller with the "trivial" static controller $u = u^*$.

Let's start by checking the validity of item 1) of Theorem 2, i.e., asymptotic stability of the closed-loop system at (x^*, u^*) for any positive controller gains k_1 and k_2. Fig. 2 shows the closed-loop trajectories with respect to four different pairs of k_1 and k_2. The threshold for the switching condition is chosen as $\varepsilon = 1$ and the initial condition is $(x(0), u(0)) = ((131.37, 361), 0.2132)$. As expected, the closed-loop trajectories converge to the equilibrium point $(x^*, u^*) = ((119.4286, 380), 0.2632)$.

Now, we choose the control design parameters as $k_1 = 0.1$, $k_2 = 6.06 \times 10^6$, $\varepsilon = 1$, and check items 2) and 3) of Theorem 2. The condition (14) for a level set Ω_c is

$$c \leq \frac{k_2}{2k_1}(u^*)^2 = 2.1 \times 10^6, \quad c < \frac{E^2}{2L} = 35 \times 10^6.$$

Let $\hat{c} = \min\{2.1 \times 10^6, 35 \times 10^6\}$, then $\Omega_{\hat{c}} \subset (\mathbb{R}^n \times \mathbb{R}^n_{>0}) \times [0, 1)^n$ is a feasible region of attraction. Note however that, according to Remark 3, $c_l = 35 \times 10^6 - \varepsilon_l$ gives a larger feasible region of attraction Ω_{c_l} for any sufficiently small $\varepsilon_l > 0$; we select in simulation $\varepsilon_l = 10^{-3}$. As can be observed from Figs. 3 and 4, both $\Omega_{\hat{c}}$ and Ω_{cl} are contained in $(\mathbb{R}^n \times \mathbb{R}^n_{>0}) \times [0, 1)^n$, which validates item 3) of Theorem 2. In particular, Fig. 3 shows that Ω_{c_l} is bounded by the surfaces $u = 0$ and $u = 1$. Fig. 4 shows the projection of $\Omega_{\hat{c}}$ and Ω_{c_l} on the x_1–x_2 plane. One can note that for any c (slightly) larger than c_l, the level set Ω_c would cross the surface $x_2 = 0$, i.e., the surface on which the voltage is equal to zero. This

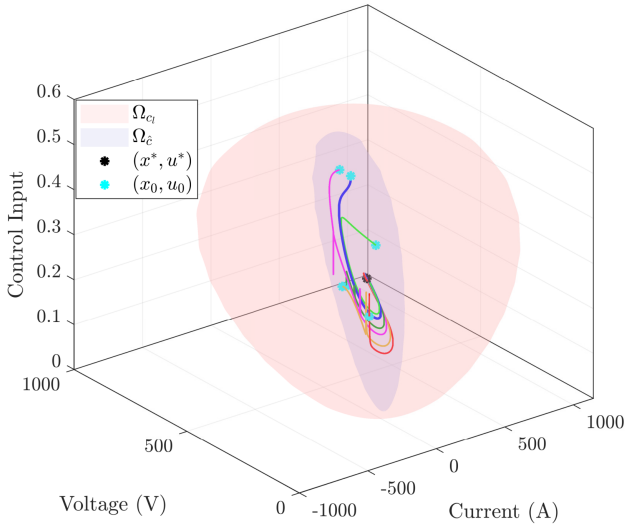

Fig. 3. Feasible regions of attraction $\Omega_{\hat{c}}$ and Ω_{c_l} and closed-loop trajectories starting from $\Omega_{\hat{c}}$.

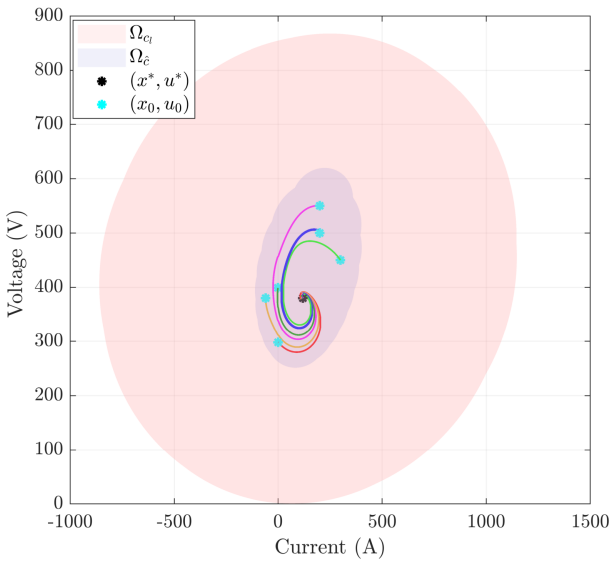

Fig. 4. Projection of $\Omega_{\hat{c}}$, Ω_{c_l} and the closed-loop trajectories on the x_1–x_2 (current–voltage) plane.

validates the necessity and sufficiency of item 3) in Theorem 2. Next, we check the validity of item 2) of Theorem 2 by focusing on $\Omega_{\hat{c}}$. As shown in Figs. 3 and 4, all the trajectories starting from $\Omega_{\hat{c}}$ remain in $\Omega_{\hat{c}}$ and converge to (x^*, u^*).

Now, in order to show the validity of the tuning rule provided in Remark 3, we repeat the simulation in Figs. 3 and 4 with the controller gains k_1 and k_2 satisfying (22), i.e., $k_1 = 0.1$ and $k_2 = 10.1 \times 10^7$. This implies $\hat{c} = c_l = 35 \times 10^6 - \varepsilon_l, \varepsilon_l = 10^{-3}$. The projection of the level set $\Omega_{\hat{c}}$ and the trajectories of the closed-loop system on the x_1–x_2 plane are shown in Fig. 5. The trajectories start from six different initial conditions contained in $\Omega_{\hat{c}}$ and converge to (x^*, u^*), remaining inside $\Omega_{\hat{c}}$ all the time.

Now, we have a close look at the switching mechanism employed in the proposed control scheme (12). Fig. 6 shows the closed-loop trajectories starting from four different initial

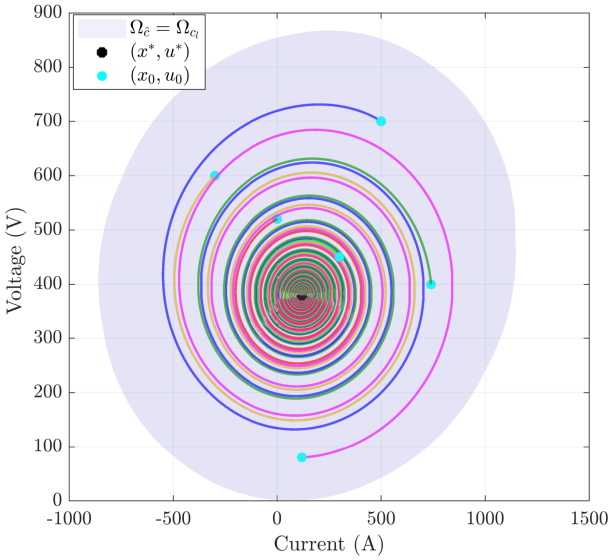

Fig. 5. Projection of $\Omega_{\hat{c}}$ and the closed-loop trajectories on the x_1–x_2 (current–voltage) plane, with the controller gains satisfying (22).

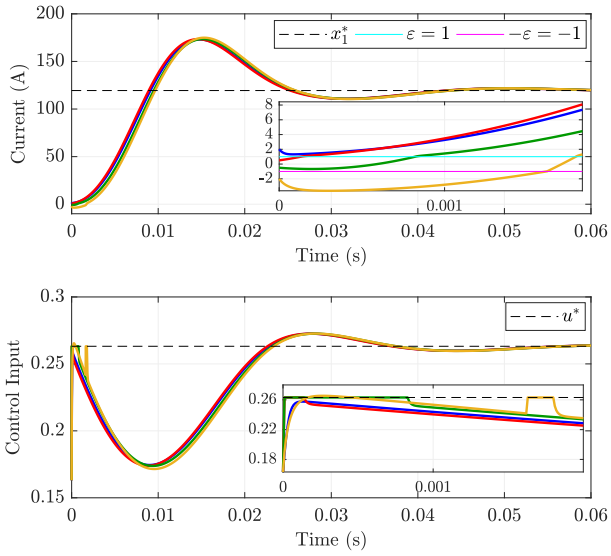

Fig. 6. Time evolution of the currents and control signals, with visualization of the switching mechanism effects.

conditions in $\Omega_{\hat{c}}$, which are selected in order to cross the switching region. It can be observed that the switching mechanism is triggered whenever the current trajectories cross the switching lines $x_1 = \varepsilon$ or $x_1 = -\varepsilon$.

Finally, we compare the performance of the proposed dynamic controller (12) with the "trivial" static controller $u = u^*$. Fig. 7 shows the closed-loop trajectories obtained with both controllers starting from two different initial conditions. Regardless of the initial condition, the closed-loop system with $u = u^*$ suffers from many more oscillations than when using the proposed controller.

B. Two-Node Case

We consider now a dc microgrid with two boost converters interconnected through a resistive–inductive power line

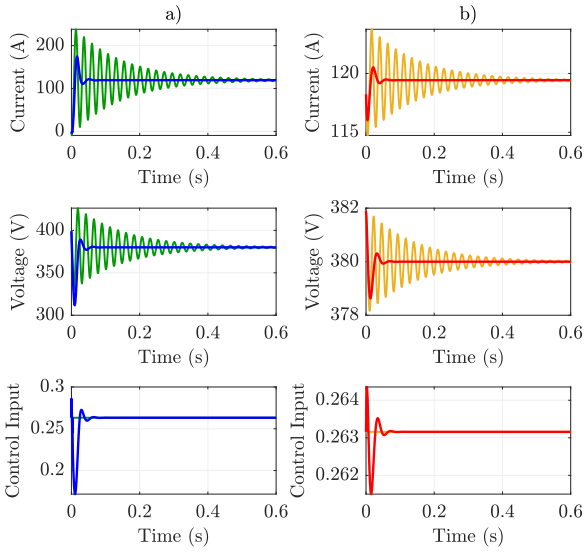

Fig. 7. Closed-loop trajectories with the proposed dynamic control scheme (black and red) and the "trivial" static controller $u = u^*$ (green and orange). a) $(x(0), u(0)) = (-0.59, 399, 0.2632)$, b) $(x(0), u(0)) = (118.23, 381.9, 0.2632)$.

(see [17], [19], [42]), i.e., we consider the microgrid model (2) with $n = 2$ and $m = 1$. Note that, for the sake of notation simplicity, we consider two identical boost converters, and all the values of the system parameters are given in Table I. Namely, we consider the system

$$\begin{aligned} L\dot{x}_{1,1} &= -(1-u_1)\,x_{2,1} + E_1 \\ L\dot{x}_{1,2} &= -(1-u_2)\,x_{2,2} + E_2 \\ C\dot{x}_{2,1} &= (1-u_1)\,x_{1,1} - I_1 - x_{2,1}/R_1 - x_3 \\ C\dot{x}_{2,2} &= (1-u_2)\,x_{1,2} - I_2 - x_{2,2}/R_2 + x_3 \\ L_p\dot{x}_3 &= \left(x_{2,1} - x_{2,2}\right) - R_p x_3. \end{aligned} \tag{27}$$

As in the previous section, we first check the validity of the items 1)–3) of Theorem 2 in the network case and then evaluate the closed-loop performance by considering two different scenarios based on the experimental tests in [17] and [19].

First, we show the asymptotic stability of the closed-loop system at the desired equilibrium point (x^*, u^*) for any positive gains $k_{1,i}$ and $k_{2,i}$, $i = 1, 2$. Specifically, Fig. 8 shows the closed-loop trajectories with the control gains selected as

$$\begin{aligned} (k_{1,1}, k_{2,1}) &= (0.1, 6.06 \times 10^6) \\ (k_{1,2}, k_{2,2}) &= (1, 5 \times 10^7). \end{aligned}$$

These values have been chosen through a trial and error procedure to get both a large feasible region of attraction and desired transient performance. More precisely, the feasible region of attraction is $\Omega_{\hat{c}}$, with $\hat{c} = 1.7313 \times 10^6$ satisfying (14). The switching condition is defined by the thresholds $\varepsilon_1 = \varepsilon_2 = 1$ and the initial conditions are

$$\begin{aligned} \left(x_{1,1}(0), x_{2,1}(0), u_1(0)\right) &= (95.542, 383.8, 0.1632)) \\ \left(x_{1,2}(0), x_{2,2}(0), u_2(0)\right) &= (143.314, 380, 0.2632) \\ x_3(0) &= 0. \end{aligned}$$

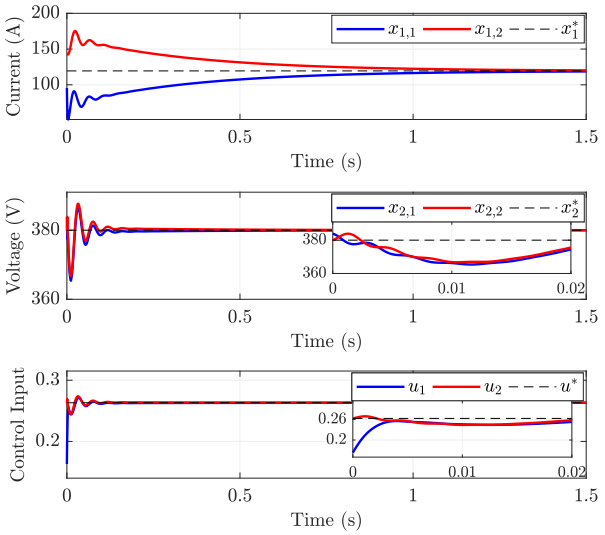

Fig. 8. Closed-loop trajectories starting from a feasible region of attraction $\Omega_{\hat{c}}$.

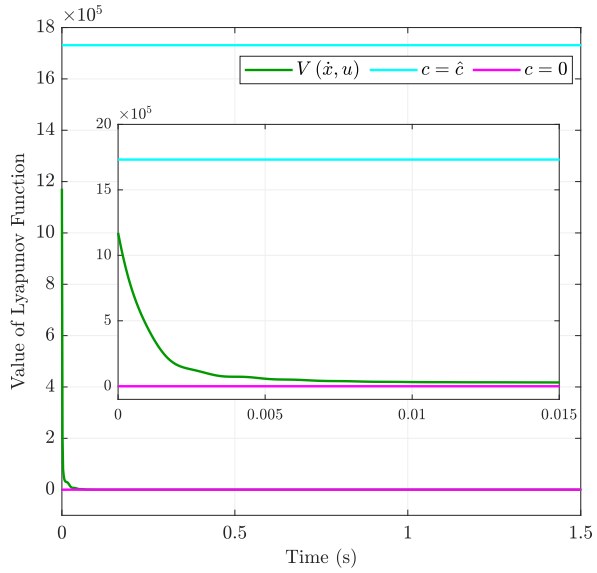

Fig. 9. Time evolution of the Lyapunov function (15).

As expected, the closed-loop trajectories converge to the desired equilibrium point, i.e.,

$$\begin{aligned}\left(x_{1,1}^*, x_{2,1}^*, u_1^*\right) &= (119.42, 380, 0.2632)\\ \left(x_{1,2}^*, x_{2,2}^*, u_2^*\right) &= (119.42, 380, 0.2632)\\ x_3^* &= 0.\end{aligned}$$

Moreover, since the above initial conditions belong to $\Omega_{\hat{c}}$, as expected, the closed-loop trajectories converge to the desired equilibrium point (x^*, u^*) while fulfilling the physical constraints, i.e., voltages are positive and the control signals belong to the interval $[0, 1)$ all the time (see Fig. 8). Fig. 9 shows the time evolution of the Lyapunov function $V(x(t), u(t))$ in (15), which satisfies $V(x(t), u(t)) \leq \hat{c}$ for all $t \geq 0$. Furthermore, $V(x(t), u(t))$ converges to 0, and thus $\Omega_{\hat{c}}$ is a feasible region of attraction.

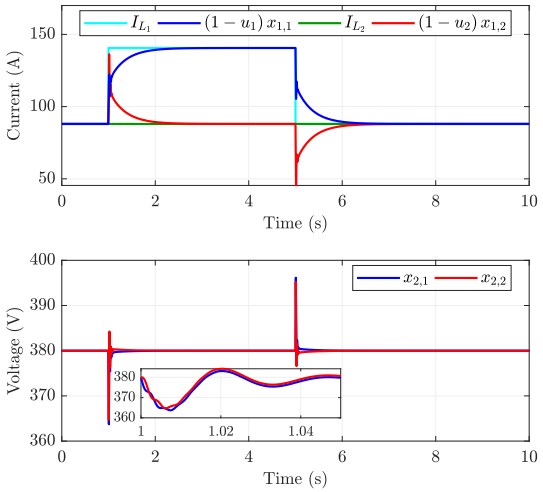

Fig. 10. Closed-loop trajectories considering a step variation of 20 kW in node 1.

Now, we further assess the performance of the proposed controller (12) considering two different scenarios as in [17] and [19].

Scenario I: In this scenario, we evaluate the closed-loop performance when a step variation occurs in the power absorbed by the load or the power generated, e.g., by a photovoltaic plant, i.e., we consider step variations of the current $I_{L,i} = I_i + x_{2,i}/R_i$, $i = 1, 2$. Let each node of the dc microgrid (27) represent for instance a battery regulating its output voltage toward the desired reference $x_{2,i}^* = 380$ V. Specifically, let the power demand in node 1 increase by 20 kW at the time instant $t = 1$ s until the time instant $t = 5$ s. As shown in Fig. 10, the proposed dynamic controller asymptotically stabilizes the dc microgrid at the desired equilibrium point (x^*, u^*) after a short transient during which the voltage deviation is about 4% of the desired value, thus satisfying, for example, the standards for dc networks used for powering of telecommunication applications [43], where tolerance of 10% (with respect to the desired values) is considered acceptable. This shows the robustness of the proposed controller with respect to unknown loads. This scenario is repeated by considering a step variation of 20 kW in the power generated, e.g., by a photovoltaic plant, which is simulated by implementing a negative variation of the current $I_{L,1}$. The results are shown in Fig. 11 and comments similar to the ones above hold. In addition, we would like to remark that the amplitude of the overshoots and undershoots at the time instants $t = 1$ s and $t = 5$ s in Figs. 10 and 11 depends on the amplitude of the load variations.

Scenario II: In this scenario, we evaluate the closed-loop performance by considering step changes of the desired voltage. At the time instant $t = 1$ s, the desired voltage for node 1 changes from $x_{2,1}^* = 380$ V to $x_{2,1}^* = 375$ V. Then, after 4 s, also the desired voltage for node 2 changes from $x_{2,2}^* = 380$ V to $x_{2,2}^* = 375$ V. As shown in Fig. 12, the proposed control scheme tracks the voltage reference, and the dc microgrid is stabilized at the desired equilibrium point (x^*, u^*).

C. Multinode DC Network

To show the performance of the proposed controller (12) in a more realistic scenario, we consider a dc network consisting

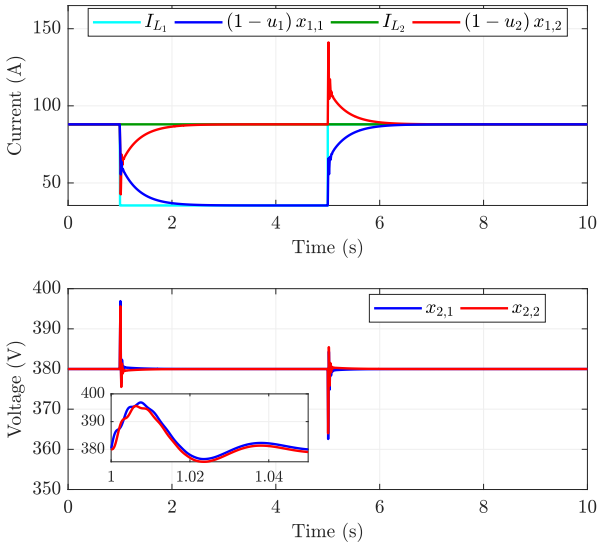

Fig. 11. Closed-loop trajectories considering a step variation of −20 kW in node 1.

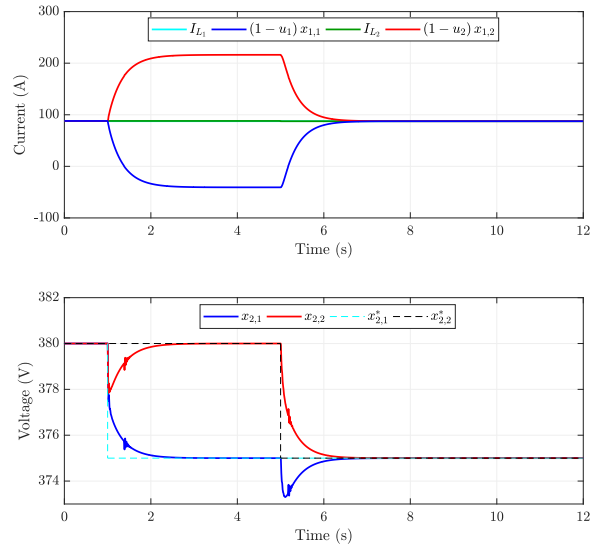

Fig. 12. Closed-loop trajectories considering step variations of the voltage reference.

of four nodes in a ring configuration with ZIP loads, i.e.,

$$L\dot{x}_1 = -(\mathbb{1}_n - u)\circ x_2 + E \tag{28a}$$

$$C\dot{x}_2 = (\mathbb{1}_n - u)\circ x_1 - I - R^{-1}x_2 - [x_2]^{-1}P + Dx_3 \tag{28b}$$

$$L_p\dot{x}_3 = -D^\top x_2 - R_p x_3 \tag{28c}$$

where the incidence matrix $D \in \mathbb{R}^{4\times 4}$ is as follows:

$$D = \begin{pmatrix} -1 & 0 & 0 & 1 \\ 1 & -1 & 0 & 0 \\ 0 & 1 & -1 & 0 \\ 0 & 0 & 1 & -1 \end{pmatrix}.$$

The values of the system parameters are given in Table I, while the CPLs are selected as $P = (2, 2, 5, 0)$ kW. We consider the

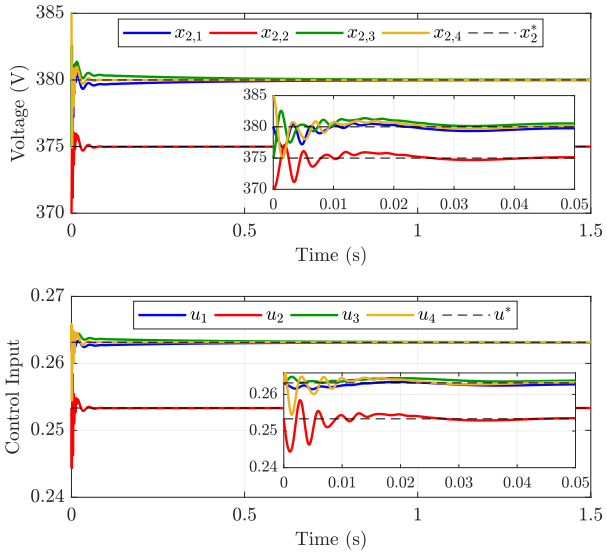

Fig. 13. Closed-loop trajectories of a multinode dc network.

following equilibrium points:

$$\begin{aligned}
(x_{1,1}^*, x_{2,1}^*, u_1^*) &= (300.56, 380, 0.2632)\\
(x_{1,2}^*, x_{2,2}^*, u_2^*) &= (-219.07, 375, 0.2533)\\
(x_{1,3}^*, x_{2,3}^*, u_3^*) &= (311.27, 380, 0.2632)\\
(x_{1,4}^*, x_{2,4}^*, u_4^*) &= (119.42, 380, 0.2632)
\end{aligned}$$

where the reference voltages are not identical for all the nodes. Then, by setting the controller gains as

$$\begin{aligned}
(k_{1,1}, k_{2,1}) &= (0.1, 6.06\times 10^6), \quad (k_{1,2}, k_{2,2}) = (1, 5\times 10^7)\\
(k_{1,3}, k_{2,3}) &= (0.1, 6.06\times 10^6), \quad (k_{1,4}, k_{2,4}) = (1, 5\times 10^7)
\end{aligned}$$

the level set Ω_c, with $c = 1.6\times 10^6$ satisfying (25), is the estimated feasible domain of attraction.

Consider the following initial conditions:

$$\begin{aligned}
(x_{1,1}(0), x_{2,1}(0), u_1(0)) &= (270.50, 380, 0.2632)\\
(x_{1,2}(0), x_{2,2}(0), u_2(0)) &= (-219.07, 370, 0.2533)\\
(x_{1,3}(0), x_{2,3}(0), u_3(0)) &= (342.40, 375, 0.2632)\\
(x_{1,4}(0), x_{2,4}(0), u_4(0)) &= (119.42, 385, 0.2632).
\end{aligned}$$

Then, the time evolution of the voltages and control signals are depicted in Fig. 13, showing that all trajectories converge to the desired equilibrium point while satisfying the physical constraints of the network.

V. Conclusion and Future Research

In this article, we design a fully decentralized dynamic control system to regulate the voltage in a boost converter-based dc microgrid. We use a Krasovskii Lyapunov function and analyze its level sets to ensure the asymptotic stability of a desired equilibrium point while satisfying predefined physical constraints. In other words, we provide an estimation of the microgrid's feasible region of attraction. Finally, we assess in simulation the proposed control scheme to validate the established theoretical results.

The proposed controller is designed by integrating a differential passivity-based controller. We are generalizing the proposed approach to differentially passive systems with integrable differentially passive outputs, which is an interesting research direction and will be explored in future work. Another interesting future research directions include investigating different candidate Lyapunov functions to get a less conservative estimation of the feasible domain of attraction. Moreover, to improve the robustness features of the control system, we are also interested in including in the control law an integral action on the voltage error and finding a suitable Lyapunov function to establish asymptotic stability of the desired equilibrium point. Finally, we are interested in extending the proposed controller to achieve also load sharing, in addition to voltage regulation.

APPENDIX
PROOF OF COROLLARY 1

Proof: The dynamics of a dc microgrid (2) with ZIP loads read as follows:

$$L\dot{x}_1 = -(\mathbb{1}_n - u) \circ x_2 + E \tag{29a}$$

$$C\dot{x}_2 = (\mathbb{1}_n - u) \circ x_1 - I - R^{-1}x_2 - [x_2]^{-1} P + Dx_3 \tag{29b}$$

$$L_p\dot{x}_3 = -D^\top x_2 - R_p x_3. \tag{29c}$$

For a given $E \leq x_2^* \in \mathcal{R}$, where the set $\mathcal{R}$ is defined in (24), the equilibrium point corresponding to dynamics (29) is denoted by $x^* = (x_1^{*\top}, x_2^{*\top}, x_3^{*\top})^\top$. Now, let us consider the Lyapunov function $V(\dot{x}, u)$ given in (10). The time derivative of $V(\dot{x}, u)$ along the trajectories of the system (29) in closed-loop with the controller (12) satisfies the following inequality:

$$\dot{V}(\dot{x}, u) < -\sum_{i=1}^{q} k_{1,i}^{-1}\varepsilon_i x_{2,i}\dot{u}_i^2 - \dot{x}_2^\top \left(R^{-1} - [x_2]^{-2} P\right)\dot{x}_2 - \dot{x}_3^\top R_p \dot{x}_3 \tag{30}$$

which is negative semi-definite at (x^*, u^*) on the set $(\mathbb{R}^n \times \mathcal{R}^n \times \mathbb{R}^m) \times [0, 1)^n$. Hence, the stability of the equilibrium point (x^*, u^*) is proved. To show the asymptotic stability of (x^*, u^*), we invoke LaSalle's invariance principle on the compact set Ω_c defined in (13) for a suitable $c > 0$ such that $\Omega_c \subset (\mathbb{R}^n \times \mathcal{R}^n \times \mathbb{R}^m) \times [0, 1)^n$. Therefore, also the asymptotic stability of the equilibrium point is proved with the set Ω_c being the estimated feasible domain of attraction of the desired equilibrium point.

In order to estimate a feasible region of attraction, we notice that the inequality (25a) is identical to the first inequality in (14). Therefore, the proof to show the correctness of (25a) is the same as the proof of Theorem 2. For the inequality (25b), we follow the same steps as in the proof of Theorem 2, i.e., we aim to obtain the tightest level set Ω_c contained in the region bounded by the line $x_{2,i} = (\beta_{1,i}\beta_{2,i})^{1/2}$. From the quadratic structure of $V(\dot{x}, u)$, it follows that the set $\Omega_{c_{x_{2,(\beta_{1,i}\beta_{2,i})^{1/2},i}}}$ is tangent to the line $x_{2,i} = (\beta_{1,i}\beta_{2,i})^{1/2}$ if and only if the inequality (25b) holds. Finally, we observe that for ZI loads, since $\beta_{1,i} = 0$ for all $i \in \mathcal{V}$, then the inequality (25b) becomes identical to the second inequality in (14). ■

REFERENCES

[1] J. M. Guerrero et al., "Distributed generation: Toward a new energy paradigm," *IEEE Ind. Electron. Mag.*, vol. 4, no. 1, pp. 52–64, Mar. 2010.

[2] N. L. Panwar, S. C. Kaushik, and S. Kothari, "Role of renewable energy sources in environmental protection: A review," *Renew. Sustain. Energy Rev.*, vol. 15, no. 3, pp. 1513–1524, Apr. 2011.

[3] T. Ackermann, G. Andersson, and L. Söder, "Distributed generation: A definition," *Electr. Power Syst. Res.*, vol. 57, no. 3, pp. 195–204, 2001.

[4] N. Hatziargyriou, *Microgrids: Architectures and Control*. Hoboken, NJ, USA: Wiley, 2014.

[5] J. E. Machado, S. Ahmed, J. M. A. Scherpen, and M. Cucuzzella, "Robust, distributed and optimal control of smart grids," in *Proc. EPJ Web Conf.*, vol. 268, 2022, p. 00016.

[6] J. Schiffer, R. Ortega, A. Astolfi, J. Raisch, and T. Sezi, "Conditions for stability of droop-controlled inverter-based microgrids," *Automatica*, vol. 50, no. 10, pp. 2457–2469, Oct. 2014.

[7] J. W. Simpson-Porco, F. Dörfler, and F. Bullo, "Voltage stabilization in microgrids via quadratic droop control," *IEEE Trans. Autom. Control*, vol. 62, no. 3, pp. 1239–1253, Mar. 2017.

[8] M. Cucuzzella, G. P. Incremona, and A. Ferrara, "Decentralized sliding mode control of islanded AC microgrids with arbitrary topology," *IEEE Trans. Ind. Electron.*, vol. 64, no. 8, pp. 6706–6713, Aug. 2017.

[9] M. Cucuzzella, S. Trip, A. Ferrara, and J. Scherpen, "Cooperative voltage control in AC microgrids," in *Proc. IEEE Conf. Decis. Control (CDC)*, Dec. 2018, pp. 6723–6728.

[10] S. Feng, M. Cucuzzella, T. Bouman, L. Steg, and J. M. A. Scherpen, "An integrated human–cyber–physical framework for control of microgrids," *IEEE Trans. Smart Grid*, vol. 14, no. 5, pp. 3388–3400, Sep. 2023.

[11] T. Dragicevic, X. Lu, J. C. Vasquez, and J. M. Guerrero, "DC microgrids—Part I: A review of control strategies and stabilization techniques," *IEEE Trans. Power Electron.*, vol. 31, no. 7, pp. 4876–4891, Jul. 2016.

[12] J. J. Justo, F. Mwasilu, J. Lee, and J.-W. Jung, "AC-microgrids versus DC-microgrids with distributed energy resources: A review," *Renew. Sustain. Energy Rev.*, vol. 24, pp. 387–405, Aug. 2013.

[13] E. Planas, J. Andreu, J. I. Gárate, I. M. De Alegría, and E. Ibarra, "AC and DC technology in microgrids: A review," *Renew. Sustain. Energy Rev.*, vol. 43, pp. 726–749, Mar. 2015.

[14] D. Jeltsema and J. M. A. Scherpen, "Tuning of passivity-preserving controllers for switched-mode power converters," *IEEE Trans. Autom. Control*, vol. 49, no. 8, pp. 1333–1344, Aug. 2004.

[15] M. S. Sadabadi, Q. Shafiee, and A. Karimi, "Plug-and-play robust voltage control of DC microgrids," *IEEE Trans. Smart Grid*, vol. 9, no. 6, pp. 6886–6896, Nov. 2018.

[16] M. Cucuzzella, S. Trip, C. De Persis, X. Cheng, A. Ferrara, and A. van der Schaft, "A robust consensus algorithm for current sharing and voltage regulation in DC microgrids," *IEEE Trans. Control Syst. Technol.*, vol. 27, no. 4, pp. 1583–1595, Jul. 2019.

[17] M. Cucuzzella, R. Lazzari, S. Trip, S. Rosti, C. Sandroni, and A. Ferrara, "Sliding mode voltage control of boost converters in DC microgrids," *Control Eng. Pract.*, vol. 73, pp. 161–170, Apr. 2018.

[18] A. Iovine and F. Mazenc, "Bounded control for DC/DC converters: Application to renewable sources," in *Proc. IEEE Conf. Decis. Control (CDC)*, Dec. 2018, pp. 3415–3420.

[19] M. Cucuzzella, R. Lazzari, Y. Kawano, K. C. Kosaraju, and J. M. A. Scherpen, "Robust passivity-based control of boost converters in DC microgrids," in *Proc. IEEE 58th Conf. Decis. Control (CDC)*, Dec. 2019, pp. 8435–8440.

[20] P. Monshizadeh, J. E. Machado, R. Ortega, and A. van der Schaft, "Power-controlled Hamiltonian systems: Application to electrical systems with constant power loads," *Automatica*, vol. 109, Nov. 2019, Art. no. 108527.

[21] J. E. Machado et al., "An adaptive observer-based controller design for active damping of a DC network with a constant power load," *IEEE Trans. Control Syst. Technol.*, vol. 29, no. 6, pp. 2312–2324, Nov. 2021.

[22] A. Silani, M. Cucuzzella, J. M. A. Scherpen, and M. J. Yazdanpanah, "Robust output regulation for voltage control in DC networks with time-varying loads," *Automatica*, vol. 135, Jan. 2022, Art. no. 109997.

[23] M. Cucuzzella, K. C. Kosaraju, and J. M. A. Scherpen, "Voltage control of DC microgrids: Robustness for unknown ZIP-loads," *IEEE Control Syst. Lett.*, vol. 7, pp. 139–144, 2023.
[24] M. Nazari Monfared, Y. Kawano, and M. Cucuzzella, "Voltage control of boost converters: Feasibility guarantees," *IFAC-PapersOnLine*, vol. 56, no. 2, pp. 803–808, 2023.
[25] Z. Fu, M. Cucuzzella, C. Cenedese, W. Yu, and J. M. Scherpen, "A distributed control framework for the optimal operation of DC microgrids," in *Proc. IEEE 61st Conf. Decis. Control (CDC)*, Dec. 2022, pp. 4585–4590.
[26] J. Ferguson, M. Cucuzzella, and J. M. A. Scherpen, "Increasing the region of attraction in DC microgrids," *Automatica*, vol. 151, May 2023, Art. no. 110883.
[27] D. Zonetti, G. Bergna-Diaz, R. Ortega, and N. Monshizadeh, "PID passivity-based droop control of power converters: Large-signal stability, robustness and performance," *Int. J. Robust Nonlinear Control*, vol. 32, no. 3, pp. 1769–1795, 2022.
[28] A. Martinelli, P. Nahata, and G. Ferrari-Trecate, "Voltage stabilization in MVDC microgrids using passivity-based nonlinear control," in *Proc. IEEE Conf. Decis. Control (CDC)*, Dec. 2018, pp. 7022–7027.
[29] J. Moreno-Valenzuela and O. García-Alarcón, "On control of a boost DC–DC power converter under constrained input," *Complexity*, vol. 2017, no. 1, 2017, Art. no. 4143901.
[30] M. Shafiee-Rad, M. S. Sadabadi, Q. Shafiee, and M. R. Jahed-Motlagh, "Robust performance satisfaction of DC microgrids using a decentralized optimal voltage control strategy," *IEEE Syst. J.*, vol. 16, no. 1, pp. 464–474, Mar. 2022.
[31] P. Hippe, *Windup in Control: Its Effects and Their Prevention*. Springer, 2006.
[32] R. Cisneros, R. Ortega, C. A. Beltrán, D. Langarica-Córdoba, and L. H. Díaz-Saldierna, "Output voltage regulation of a fuel cell/boost converter system: A PI-PBC approach," 2023, *arXiv:2302.08697*.
[33] K. C. Kosaraju, M. Cucuzzella, J. M. A. Scherpen, and R. Pasumarthy, "Differentiation and passivity for control of Brayton–Moser systems," *IEEE Trans. Autom. Control*, vol. 66, no. 3, pp. 1087–1101, Mar. 2021.
[34] Y. Kawano, K. C. Kosaraju, and J. M. A. Scherpen, "Krasovskii and shifted passivity-based control," *IEEE Trans. Autom. Control*, vol. 66, no. 10, pp. 4926–4932, Oct. 2021.
[35] Y. Kawano, M. Cucuzzella, S. Feng, and J. M. A. Scherpen, "Krasovskii and shifted passivity based output consensus," *Automatica*, vol. 155, Sep. 2023, Art. no. 111167.
[36] Y. Kawano, M. Cucuzzella, and J. M. A. Scherpen, "Krasovskii and shifted passivity approaches to mixed Input/Output consensus," *IEEE Control Syst. Lett.*, vol. 7, pp. 1951–1956, 2023.
[37] R. D. Middlebrook and S. Ćuk, "A general unified approach to modelling switching-converter power stages," *Int. J. Electron. Theor. Exp.*, vol. 42, no. 6, pp. 521–550, 1977.
[38] A. J. van der Schaft, "On differential passivity," *IFAC Proc. Volumes*, vol. 46, no. 23, pp. 21–25, 2013.
[39] Y. Kawano and B. Besselink, "Incremental versus differential approaches to exponential stability and passivity," *IEEE Trans. Autom. Control*, pp. 1–8, 2024, doi: 10.1109/TAC.2024.3385036.
[40] F. Forni, R. Sepulchre, and A. J. van der Schaft, "On differential passivity of physical systems," in *Proc. 52nd IEEE Conf. Decis. Control*, Dec. 2013, pp. 6580–6585.
[41] H. K. Khalil, *Nonlinear Systems*, vol. 115, 3rd ed. Upper Saddle River, NJ, USA: Prentice-Hall, 2002.
[42] D. Ronchegalli and R. Lazzari, "Development of the control strategy for a direct current microgrid: A case study," in *Proc. AEIT Int. Annu. Conf. (AEIT)*, Oct. 2016, pp. 1–6.
[43] W. Schulz, "ETSI standards and guides for efficient powering of telecommunication and datacom," in *Proc. 29th Int. Telecommun. Energy Conf. (INTELEC)*, Sep./Oct. 2007, pp. 168–173.

Morteza Nazari Monfared is currently pursuing the Ph.D. degree in electronics, computer science, and electrical engineering in the field of systems and control with the University of Pavia, Pavia, Italy.

He is a member of the Identification and Control of Dynamic Systems (ICDS) Laboratory, University of Pavia, and works under the supervision of Prof. Michele Cucuzzella. He also was a Visiting Ph.D. Student at the University of Groningen, Groningen, The Netherlands. His research interests include nonlinear control systems and passivity theory with their applications to smart energy and power networks.

Yu Kawano (Member, IEEE) received the M.S. and Ph.D. degrees in engineering from Osaka University, Osaka, Japan, in 2011 and 2013, respectively.

He has been an Associate Professor with the Graduate School of Advanced Science and Engineering, Hiroshima University, Higashihiroshima, Japan, since 2019. Following this, he was a Post-Doctoral Researcher at Kyoto University, Japan, before relocating to the University of Groningen, Groningen, The Netherlands, in 2016. He has held visiting research positions at Tallinn University of Technology, Tallinn, Estonia, the University of Groningen, and the University of Pavia, Pavia, Italy. His research interests include nonlinear systems, complex networks, model reduction, and privacy of control systems.

Dr. Kawano is currently a member of the EUCA Conference Editorial Board and an Associate Editor for *Systems and Control Letters*.

Michele Cucuzzella (Member, IEEE) received the M.Sc. degree (Hons.) in electrical engineering and the Ph.D. degree in systems and control from the University of Pavia, Pavia, Italy, in 2014 and 2018, respectively.

From 2017 to 2020, he was a Post-Doctoral Researcher at the University of Groningen (UG), Groningen, The Netherlands. He then joined the University of Pavia as an Assistant Professor. In 2024, he moved to the Engineering and Technology Institute Groningen, Faculty of Science and Engineering, UG, as an Associate Professor. He is also a Visiting Associate Professor at Hiroshima University, Higashihiroshima, Japan. He has co-authored the book *Advanced and Optimization Based Sliding Mode Control: Theory and Applications* (SIAM, 2019). His research activities are mainly in the area of nonlinear control with application to the energy domain and smart complex systems.

Dr. Cucuzzella is a member of the EUCA Conference Editorial Board and the IEEE CSS Technology Conferences Editorial Board. He received the Certificate of Outstanding Service as a reviewer of the IEEE CONTROL SYSTEMS LETTERS 2019. He also received the 2020 IEEE TRANSACTIONS ON CONTROL SYSTEMS TECHNOLOGY Outstanding Paper Award, the IEEE Italy Section Award for the best Ph.D. thesis on new technological challenges in energy and industry, and the SIDRA Award for the best Ph.D. thesis in the field of systems and control engineering. He was also the Finalist for the EECI Award for the best Ph.D. thesis in Europe in the field of control for complex and heterogeneous systems and the IEEE-CSS Italy Best Young Paper Award. He has been serving as an Associate Editor for the *European Journal of Control* since 2022.

Open Access funding provided by 'Università degli Studi di Pavia' within the CRUI CARE Agreement